CRISPRi is not strand-specific and redefines the transcriptional landscape

Françoise S. Howe[1], Andrew Russell[1], Afaf El-Sagheer[2,3], Anitha Nair[1], Tom Brown[2] and Jane Mellor[1]*.

[1] Department of Biochemistry, University of Oxford, South Parks Road, Oxford, OX1 3QU, UK

[2] Department of Chemistry, Chemistry Research Laboratory, University of Oxford, South Parks Road, Oxford, OX1 3TA, UK

[3] Chemistry Branch, Faculty of Petroleum and Mining Engineering, Suez University, Suez 43721, Egypt.

* Correspondence: jane.mellor@bioch.ox.ac.uk

ABSTRACT

CRISPRi, an adapted CRISPR-Cas9 system, is proposed to act as a strand-specific roadblock to repress transcription in eukaryotic cells using guide RNAs (sgRNAs) to target catalytically inactive Cas9 (dCas9) and offers an alternative to genetic interventions for studying pervasive antisense transcription. Here we successfully use click chemistry to construct DNA templates for sgRNA expression and show, rather than acting simply as a roadblock, binding of sgRNA/dCas9 creates an environment that is permissive for transcription initiation and termination, thus generating novel sense and antisense transcripts. At *HMS2* in *Saccharomyces cerevisiae*, sgRNA/dCas9 targeting to the non-template strand results in antisense transcription termination, premature termination of a proportion of sense transcripts and initiation of a novel antisense transcript downstream of the sgRNA/dCas9 binding site. This redefinition of the transcriptional landscape by CRISPRi demonstrates that it is not strand-specific and highlights the controls and locus understanding required to properly interpret results from CRISPRi interventions.

25 **INTRODUCTION**

26   Eukaryotic genomes are pervasively transcribed but the effect of this inter- and intragenic

27   transcription is not fully understood (Mellor, Woloszczuk, & Howe, 2016). Of particular interest is the

28   function of antisense transcription, which alters the chromatin in the vicinity of sense promoters

29   (Lavender et al., 2016; Murray et al., 2015; Pelechano & Steinmetz, 2013), and is associated with

30   repression, activation or no change in levels of the corresponding sense transcript (Murray et al.,

31   2015). Discerning the mechanism by which antisense transcription functions in gene regulation is

32   confounded by the difficulty in ablating antisense transcription without direct genetic intervention

33   (Bassett et al., 2014). A new approach, CRISPR interference (CRISPRi) (Qi et al. 2013), can circumvent

34   these issues by avoiding the need to manipulate endogenous DNA sequences. An

35   endonucleolytically dead version of Cas9 (dCas9) is recruited by single base pairing guide RNAs

36   (sgRNAs) targeting the non-template (NT) DNA strand, where it blocks transcription strand-

37   specifically at the loci tested (Lenstra, Coulon, Chow, & Larson, 2015; Qi et al., 2013). In a further

38   adaptation, dCas9 fusion with transcriptional repressors or activators allows both negative and

39   positive regulation of transcription respectively (Gilbert et al., 2013, 2014), but the strand-specificity

40   is lost and thus is not suitable for strand-specific repression of antisense transcription. The sgRNA

41   compenent of the CRISPRi system consists of two regions: a constant region (82 nt) that binds to

42   dCas9 and a variable region (20 nt) that is responsible for targeting. The modular nature of the

43   sgRNA lends itself to synthetic copper(I)-catalysed alkyne-azide cycloaddition (CuAAC) click

44   chemistry (El-Sagheer & Brown, 2010). The stable artificial triazole DNA linker generated is

45   biocompatibile, being read and accurately copied by DNA and RNA polymerases (Birts et al., 2014;

46   El-Sagheer & Brown, 2011; El-Sagheer, Sanzone, Gao, Tavassoli, & Brown, 2011). We show that click

47   chemistry is an efficient method for sgRNA construction and that when combined with dCas9, these

48   sgRNAs are as effective as sgRNAs produced from chemically synthesised full-length DNA templates

49   at reducing levels of transcripts *in vivo*. However, it is still not completely understood how the

50   CRISPRi system functions strand-specifically or why sgRNAs must target the non-template strand.

51 Here we use the CRISPRi system to study the effect of blocking antisense transcription at loci with

52 well characterised sense:antisense transcript pairs. We have previously used a promoter deletion of

53 the antisense transcript *SUT650* at the *HMS2* locus to show that *SUT650* represses *HMS2* sense

54 transcription (Nguyen et al., 2014). Now we use CRISPRi to examine the effects of blocking *SUT650*

55 antisense transcription to ask (i) whether *SUT650* represses *HMS2* sense transcription *without* a

56 genetic intervention and (ii) whether CRISPRi is strand-specific using, in addition to *HMS2*, an

57 engineered *GAL1* gene with a well characterised antisense transcript (Murray et al., 2012, 2015).

58 The main conclusion from this study is that CRISPRi at the *HMS2* locus is not fully strand-specific and

59 results in (i) premature termination of the sense transcript and (ii) initiation of a new unstable

60 antisense transcript in the vicinity of the sgRNA binding site. As transcription from this new antisense

61 initiation site extends in to the *HMS2* promoter, there is no net change in *HMS2* sense transcript

62 levels. Thus CRISPRi redefines the transcriptional landscape at *HMS2*. This suggests that routine use

63 of CRISPRi for gene expression analysis will require rigorous analysis of transcript integrity and

64 function before conclusions can be drawn.

65 **RESULTS & DISCUSSION**

66 **DNA templates for sgRNA production can be made using click chemistry**

67 CRISPRi-mediated transcriptional repression requires co-expression of a mature sgRNA and dCas9

68 (Fig 1A). A small library of single-stranded DNAs, comprised of templates for sgRNA variable regions,

69 were joined to the constant region using click chemistry (Fig. 1B) and used successfully as templates

70 for PCR, with no significantly different efficiencies when compared to control full-length synthesised

71 oligonucleotides (Fig. 1C). The PCR products were inserted in place of a *URA3* selection cassette in

72 the endogenous *snR52* locus for expression of a transcript that is then processed to form the mature

73 nuclear-retained sgRNA (Fig. 1A). Levels of dCas9 protein were uniform between strains (Fig. 1 –

74 Figure Supplement 1). Neither insertion of *URA3* into snR52 nor dCas9 expression in the control

75   strains affected growth rate, although strains expressing some sgRNAs grew more slowly indicating a

76   physiological effect (Fig. 1D).

77   **CRISPRi represses the production of antisense transcripts at *HMS2* and *GAL1***

78   CRISPRi represses transcription when sgRNAs/dCas9 are targeted to the non-template (NT) strand

79   next to a protospacer adjacent motif (PAM) (Qi et al., 2013) (Fig. 2A). Firstly, we used an engineered

80   version of *GAL1* that has a stable antisense transcript (*GAL1* AS) initiating within an *ADH1* terminator

81   inserted into the *GAL1* coding region (Murray et al., 2012) (Fig. 2B). *GAL1* AS is present in cells grown

82   in glucose-containing media when the *GAL1* gene is repressed and is reduced as cells are switched

83   into galactose-containing media and *GAL1* sense is induced (Fig. 2C lanes 1-3). We designed sgRNAs

84   adjacent to two PAM sequences on the non-template strand near the antisense transcription start

85   site (TSS) (AS+28NT and AS+112NT) and a third strand-specificity control sgRNA on the template

86   strand in this region (AS+93T) (Fig. 2B). Only sgRNA AS+112NT/dCas9 caused significant (p=0.016)

87   reduction in *GAL1* antisense transcript levels, as assessed by Northern blotting (Fig. 2C,D).

88   Next, we examined the *HMS2* locus which has a stable antisense transcript, *SUT650*, initiating within

89   the 3' coding region of *HMS2* (Nguyen et al., 2014; Pelechano, Wei, & Steinmetz, 2013). We

90   designed three *SUT650*-targeting sgRNAs, one acting as a control located 44 nucleotides upstream of

91   the *SUT650* TSS on the non-template strand (AS-44NT), and two sgRNAs, AS+148NT and AS+181NT,

92   targeting sequences downstream of the TSS (Fig. 2E). AS+148NT/dCas9 significantly (p=0.011)

93   reduced *SUT650* (Fig. 2F lanes 1&3, 2G) and this repression was comparable for the clicked and

94   control full-length synthetic constructs (Fig. 2G). However, there was no obvious effect of the other

95   two sgRNAs/dCas9 on *SUT650* levels (Fig. 2F lanes 1, 4&5, 2G). CRISPR efficiency has been linked to

96   nucleosome occupancy (Horlbeck, Witkowsky, et al., 2016; Isaac et al., 2016) but we found no

97   correlation between the level of repression and the nucleosome occupancy (Knight et al., 2014) at

98   each of the *SUT650* sgRNA target regions (Fig. 2 – Figure Supplement 1). However, other factors such

99   as sequence determinants can also influence repression (Horlbeck, Gilbert, & Villalta, 2016). These

4

100 results at *GAL1* and *HMS2* confirm CRISPRi is suitable for reducing levels of antisense transcripts in

101 yeast but controls are needed for each sgRNA designed to ensure that repression has been achieved.

CRISPRi repression of *SUT650* induces a new shorter antisense transcript at *HMS2*

103 At *HMS2*, sgRNA AS+148NT/dCas9 was able to reduce *SUT650* levels significantly (Fig. 2F,G). Since

104 *SUT650* is a substrate for the major cytoplasmic 5'-3' exonuclease Xrn1 (Fig. 2F, lanes 1&2), we

105 investigated whether the CRISPRi-induced *SUT650* reduction was due to direct repression of

106 antisense transcription and/or a reduction in *SUT650* stability. Whilst *SUT650* was not stabilised

107 upon *XRN1* deletion in the strain expressing AS+148NT/dCas9, supporting previous studies that

108 CRISPRi operates via a transcriptional block (Qi et al., 2013) (Fig. 2F, lanes 3&6, transcript B), we

109 detected a shorter antisense transcript (Fig 2F, lane 6, transcript B^t). To map transcript B^t, we used a

110 series of Northern blotting probes across the locus (Fig. 2H). With antisense-specific probes H1 and

111 H2 in the *HMS2* gene promoter and 5' coding region respectively, we could detect transcript B^t,

112 indicating that it extends into the *HMS2* sense promoter. However, probe H4 at the 3' end of the

113 *HMS2* gene was unable to hybridise to B^t, indicating that B^t initiates upstream of this site. So whilst

114 CRISPRi successfully blocked the original *SUT650*, a new Xrn1-sensitive unstable antisense transcript

115 (B^t) was created. This is potentially due to changes in the chromatin structure caused by

116 AS+148NT/dCas9 binding to this region (Horlbeck, Witkowsky, et al., 2016; Isaac et al., 2016),

117 creating an environment that is permissive for transcription initiation (Murray et al., 2012). We note

118 that using probe H4 we were also unable to detect *SUT650* initiating from its WT start site but

119 terminating at the AS+148NT binding site, due to its small size (~148 nt).

CRISPRi-induced *GAL1* AS repression does not affect the *GAL1* sense transcript

121 We tested whether *GAL1* AS repression by AS+112NT/dCas9 affected the *GAL1* sense transcript.

122 Previously we mutated a TATA-like sequence to ablate antisense transcription but observed no

123 difference in *GAL1* sense transcript levels in the population (Murray et al., 2015). Using CRISPRi, we

124 also observed no significant change in *GAL1* sense transcript levels or size (Fig. 3A,B). To support a

5

125   strand-specific transcriptional block of AS transcription, *GAL1* sense transcript polyA site usage was

126   unaffected by sgRNA AS+112NT/dCas9 (Fig. 3C). Furthermore, *XRN1* deletion in this strain also did

127   not affect polyA site usage, ruling out a partial double-stranded transcriptional block and subsequent

128   destabilisation of the resulting truncated sense transcript (Fig. 3C).

129   **CRISPRi-induced *SUT650* repression truncates the *HMS2* sense transcript**

130   Previous work shows that reducing *SUT650* transcription increases *HMS2* sense transcript levels

131   (Nguyen et al., 2014). However, blocking *SUT650* by AS+148NT/dCas9 did not similarly increase

132   *HMS2* sense levels (Fig. 3D, lanes 1&3). To our surprise, in addition to the full-length *HMS2* sense

133   transcript (A), we detected a considerably shortened *HMS2* sense transcript (A^t). Since the combined

134   levels of the truncated and full-length transcripts are similar to those in the strain not expressing an

135   sgRNA, independent of the presence of *XRN1* (Fig. 3D, lanes 1&3 or 2&6), we hypothesised that the

136   AS+148NT/dCas9 complex bound within the *HMS2* coding region may be causing partial premature

137   sense transcription termination, leading to transcript A^t. Thus, we mapped the 3' end of *HMS2* S by

138   Northern blotting using a series of strand-specific probes across the locus (Fig. 3E). Both transcripts A

139   and A^t could clearly be detected using the probes upstream of the AS+148NT/dCas9 binding site

140   (probes H1, H2, H3) but the truncated transcript was undetectable using probe H4 downstream of

141   this site. Thus the transcriptional block caused by AS+148NT/dCas9 is not strand-specific and re-

142   defines the transcriptional landscape at the *HMS2* locus by creating a chromatin environment that is

143   suitable for both transcription initiation and termination. As an additional control, we designed

144   three sgRNAs to block the *HMS2* sense transcripts (S+77NT, S+106NT, S+179NT) and monitored their

145   effects on both *HMS2* sense and antisense transcripts (Fig. 3 – Figure Supplement 1). However, we

146   observed no effect on either levels or integrity.

147   **CRISPRi-induced antisense repression at *HMS2* and *GAL1* is not as efficient as previous methods**

148   We compared the repression efficiency of CRISPRi with our previously used genetic interventions. At

149   *GAL1,* mutation of a TATA-like sequence within the *ADH1* terminator greatly reduced the level of the

150   *GAL1* antisense transcript (Fig. 4A,B) (Murray et al 2015). *XRN1* deletion in this strain only slightly

151   increased *GAL1* AS levels, suggesting that most repression was at the level of transcription rather

152   than altering transcript stability (Fig. 4B,C). By contrast, *XRN1* deletion in the strain expressing

153   AS+112NT/dCas9 did result in some upregulation of *GAL1* AS (Fig. 4B,C), indicating that antisense

154   transcript repression was not as great in this strain. Unlike at *HMS2* (Fig. 2F,G), this stabilised *GAL1*

155   AS transcript was the same size as in the control and so likely represents stabilisation of the

156   transcripts escaping repression rather than novel transcripts.

157   Next we compared the efficacy of AS+148NT/dCas9 with previous experiments to ablate *SUT650*,

158   where we replaced the entire *HMS2* coding region, including the antisense TSS with the *URA3* coding

159   region (*HMS2:URA3*) (Nguyen et al., 2014). This successful block of *SUT650* transcription increased

160   levels of the *HMS2* sense transcript, the di-cistronic *HMS2-BAT2* transcript and consequently

161   decreased levels of the downstream gene, *BAT2*, due to transcriptional interference (Fig. 4D-F).

162   Whilst CRISPRi resulted in a similar decrease in *SUT650* as *HMS2:URA3*, neither the *HMS2*, *BAT2* nor

163   *HMS2-BAT2* di-cistronic transcripts were altered (Fig. 4F). The discovery that whilst AS+148NT/dCas9

164   represses *SUT650*, a new unstable *HMS2* antisense transcript is induced and the sense transcript is

165   prematurely terminated could explain why blocking *SUT650* using CRISPRi and the *URA3* gene body

166   replacement strategies did not give the same results (Fig. 4F). Thus CRISPRi is not as effective as a

167   genetic mutation in reducing levels of either the *GAL1* or *HMS2* AS transcripts.

168   **Concluding remarks**

169   Although CRISPRi has been used to strand-specifically repress antisense transcription at *GAL10*

170   (Lenstra et al., 2015) and *GAL1* (this work), here we demonstrate that this is not true at *HMS2*. This

171   may reflect the vastly different transcription levels for the galactose inducible genes (high)

172   compared to *HMS2* (low). Furthermore, a study in human K562 cells found that CRISPRi-induced

173   repression did not correlate with which strand was targeted at 49 genes, although the mechanism

174   behind this observation was not investigated (Gilbert et al., 2014).

7

175   This work extends our previous hypothesis (Nguyen et al., 2014), allowing us to propose that, rather

176   than acting as a roadblock, the binding of the sgRNA/dCas9 complex at *HMS2* creates a new

177   chromatin environment, which is permissible for transcription initiation and termination. Thus, new

178   transcription units are generated that result in novel sense and antisense transcripts of varying

179   stabilities that are therefore not always detectable. This redefinition of the transcriptional landscape

180   highlights the levels of controls and locus understanding needed before results from using CRISPRi

181   can be interpreted.

182   **AUTHOR CONTRIBUTIONS**

183   Conception and design: FSH, AE-S, TB, JM; Acquisition of data: FSH, AR, AN; Analysis and

184   interpretation of the data: FSH, AR, AN, JM; Drafting or revising the manuscript: FSH, TB, JM;

185   Contributed unpublished, essential data, or reagents: AE-S.

186   **FUNDING**

187   The work was funded by the BBSRC (BB/J001694/2).

188   **CONFLICT OF INTEREST**

189   J.M holds stock in Oxford BioDynamics Ltd., Chronos Therapeutics Ltd., and Sibelius Ltd. but these

190   holdings present no conflict of interest with work in this article. The other authors have declared no

191   conflicts of interest.

192   **ACKNOWLEDGEMENTS**

193   The authors thank Jack Feltham for assistance with sgRNA template construction.

194

195   **REFERENCES**

196   Bassett, A. R., Akhtar, A., Barlow, D. P., Bird, A. P., Brockdorff, N., Duboule, D., … Ponting, C. P.
197   (2014). Considerations when investigating lncRNA function in vivo. *eLife*, *3*(August2014), 1–14.
198   http://doi.org/10.7554/eLife.03058

199   Birts, C. N., Sanzone, A. P., El-Sagheer, A. H., Blaydes, J. P., Brown, T., & Tavassoli, A. (2014).
200   Transcription of click-linked DNA in human cells. *Angewandte Chemie - International Edition*,
201   *53*(9), 2362–2365. http://doi.org/10.1002/anie.201308691

202   Dicarlo, J. E., Norville, J. E., Mali, P., Rios, X., Aach, J., & Church, G. M. (2013). Genome engineering in
203   Saccharomyces cerevisiae using CRISPR-Cas systems. *Nucleic Acids Research*, *41*(7), 4336–4343.
204   http://doi.org/10.1093/nar/gkt135

205   El-Sagheer, A. H., & Brown, T. (2010). Click chemistry with DNA. *Chemical Society Reviews*, *39*(4),
206   1388–1405. http://doi.org/10.1039/b901971p

207   El-Sagheer, A. H., & Brown, T. (2011). Efficient RNA synthesis by in vitro transcription of a triazole-
208   modified DNA template. *Chemical Communications (Cambridge, England)*, *47*(44), 12057–8.
209   http://doi.org/10.1039/c1cc14316f

210   El-Sagheer, A. H., Sanzone, A. P., Gao, R., Tavassoli, A., & Brown, T. (2011). Biocompatible artificial
211   DNA linker that is read through by DNA polymerases and is functional in Escherichia coli.
212   *Proceedings of the National Academy of Sciences of the United States of America*, *108*(28),
213   11338–43. http://doi.org/10.1073/pnas.1101519108

214   Gilbert, L. A., Horlbeck, M. A., Adamson, B., Villalta, J. E., Chen, Y., Whitehead, E. H., … Weissman, J.
215   S. (2014). Genome-scale CRISPR-mediated control of gene repression and activation. *Cell*,
216   *159*(3), 647–661. http://doi.org/10.1016/j.cell.2014.09.029

217   Gilbert, L. A., Larson, M. H., Morsut, L., Liu, Z., Brar, G. A., Torres, S. E., … Qi, L. S. (2013). CRISPR-
218   mediated modular RNA-guided regulation of transcription in eukaryotes. *Cell*, *154*(2), 442–451.
219   http://doi.org/10.1016/j.cell.2013.06.044

220   Horlbeck, M. A., Gilbert, L. A., & Villalta, J. E. (2016). Compact and highly active next-generation
221   libraries for CRISPR-mediated gene repression and activation. *eLife*, *9*, 1–20.
222   http://doi.org/10.7554/eLife.19760

223   Horlbeck, M. A., Witkowsky, L. B., Guglielmi, B., Replogle, J. M., Gilbert, L. A., Villalta, J. E., …
224   Weissman, J. S. (2016). Nucleosomes impede cas9 access to DNA in vivo and in vitro. *eLife*,
225   *5*(MARCH2016), 1–21. http://doi.org/10.7554/eLife.12677

226   Isaac, R. S., Jiang, F., Doudna, J. A., Lim, W. A., Narlikar, G. J., & Almeida, R. A. (2016). Nucleosome
227   breathing and remodeling constrain CRISPR-Cas9 function. *eLife*, *5*, e13450.
228   http://doi.org/10.7554/eLife.13450

229   Knight, B., Kubik, S., Ghosh, B., Bruzzone, M. J., Geertz, M., Martin, V., … Shore, D. (2014). Two
230   distinct promoter architectures centered on dynamic nucleosomes control ribosomal protein
231   gene transcription. *Genes and Development*, *28*(15), 1695–1709.
232   http://doi.org/10.1101/gad.244434.114

233   Lavender, C. A., Cannady, K. R., Hoffman, J. A., Trotter, K. W., Gilchrist, D. A., Bennett, B. D., …
234   Archer, T. K. (2016). Downstream antisense transcription predicts genomic features that define
235   the specific chromatin environment at mammalian promoters. *PLOS Genetics*, *12*(8), e1006224.
236   http://doi.org/10.1371/journal.pgen.1006224

237   Lenstra, T. L., Coulon, A., Chow, C. C., & Larson, D. R. (2015). Single-Molecule Imaging Reveals a

238   Switch between Spurious and Functional ncRNA Transcription. *Molecular Cell*, *60*, 1–14.
239   http://doi.org/10.1016/j.molcel.2015.09.028

240   Mali, P., Yang, L., Esvelt, K. M., Aach, J., Guell, M., Dicarlo, J. E., … Church, G. M. (2013). RNA-guided
241   human genome engineering via Cas9. *Science*, *339*(February), 823–827.
242   http://doi.org/10.1126/science.1232033

243   Mellor, J., Woloszczuk, R., & Howe, F. S. (2016). The Interleaved Genome. *Trends in Genetics*, *32*(1),
244   57–71. http://doi.org/10.1016/j.tig.2015.10.006

245   Murray, S. C., Haenni, S., Howe, F. S., Fischl, H., Chocian, K., Nair, A., & Mellor, J. (2015). Sense and
246   antisense transcription are associated with distinct chromatin architectures across genes.
247   *Nucleic Acids Research*, *43*(16), 7823–7837. http://doi.org/10.1093/nar/gkv666

248   Murray, S. C., Serra Barros, A., Brown, D. A., Dudek, P., Ayling, J., & Mellor, J. (2012). A pre-initiation
249   complex at the 3'-end of genes drives antisense transcription independent of divergent sense
250   transcription. *Nucleic Acids Research*, *40*(6), 2432–44. http://doi.org/10.1093/nar/gkr1121

251   Nguyen, T., Fischl, H., Howe, F. S., Woloszczuk, R., Barros, A. S., Xu, Z., … Mellor, J. (2014).
252   Transcription mediated insulation and interference direct gene cluster expression switches.
253   *eLife*, *3*, 1–21. http://doi.org/10.7554/eLife.03635

254   Pelechano, V., & Steinmetz, L. M. (2013). Gene regulation by antisense transcription. *Nature*
255   *Reviews. Genetics*, *14*(12), 880–93. http://doi.org/10.1038/nrg3594

256   Pelechano, V., Wei, W., & Steinmetz, L. M. (2013). Extensive transcriptional heterogeneity revealed
257   by isoform profiling. *Nature*, *497*(7447), 127–31. http://doi.org/10.1038/nature12121

258   Pliatsika, V., & Rigoutsos, I. (2015). "Off-Spotter": very fast and exhaustive enumeration of genomic
259   lookalikes for designing CRISPR/Cas guide RNAs. *Biology Direct*, *10*(1), 4.
260   http://doi.org/10.1186/s13062-015-0035-z

261   Qi, L. S., Larson, M. H., Gilbert, L. A., Doudna, J. A., Weissman, J. S., Arkin, A. P., & Lim, W. A. (2013).
262   Repurposing CRISPR as an RNA-guided platform for sequence-specific control of gene
263   expression. *Cell*, *152*(5), 1173–83. http://doi.org/10.1016/j.cell.2013.02.022

264

265   **MATERIALS AND METHODS**

266   **sgRNA design**

267   PAM sequences within 200 bp of the TSS in question were identified and the 20 bp immediately

268   adjacent to these were used to design the variable regions of the sgRNAs. These sequences were run

269   through an off-spotter algorithm (https://cm.jefferson.edu/Off-Spotter//) to minimise any off-target

270   effects (Pliatsika & Rigoutsos, 2015). The sequence for the engineered constant region and *SUP4*

271   terminator were taken from (Dicarlo et al., 2013; Mali et al., 2013). The *HMS2* sgRNA templates were

272   synthesised as two DNA oligonucleotides to be joined by click chemistry, with the majority of the

273   constant region on one oligonucleotide that could be used for all reactions. To increase the

274   efficiency of the click reaction, the click linkage was designed between a dCpT dinucleotide within

275   the Cas9 handle region. The sequences for the *HMS2* and *GAL1* sgRNAs are shown in Supplementary

276   File 1. Full-length sgRNA templates were also synthesised for the *GAL1* sgRNAs and as a control for

277   the *HMS2* click chemistry constructs (Eurofins Genomics).

278   **Click chemistry**

279   Single-stranded DNA oligonucleotides complementary to the constant and variable sgRNA regions

280   were synthesised by standard phosphoramidite oligonucleotide synthesis with 3'-alkyne or 5'-azido

281   modifications respectively (El-Sagheer et al., 2011) (Supplementary File 1). The click chemistry

282   reaction was performed with a Cu^1 catalyst and 24-30 nt splint DNAs (El-Sagheer et al., 2011). PCR

283   was performed for second strand synthesis, amplification and incorporation of sequences

284   homologous to the site of insertion in *S. cerevisiae*. PCR efficiencies were obtained using qPCR

285   performed three times with four serial 10-fold dilutions in triplicate (Corbett 6000 Rotorgene

286   software).

287   **Strain construction**

288   dCas9, without fusion to a transcriptional repressor domain, was expressed from a plasmid (# 46920

289   Addgene (Qi et al., 2013)) under the control of the *TDH3* promoter. The DNA templates for sgRNA

290   production were integrated in place of an exogenous *URA3* cassette immediately downstream of the

291   splice site in the endogenous *snR52* locus using homologous recombination followed by 5-FOA

292   selection. Correct insertion was confirmed by genomic DNA sequencing. *SNR52* is a Pol III-

293   transcribed C/D box small nucleolar RNA (snoRNA) gene and so does not undergo extensive post-

294   transcriptional processing such as capping and polyadenylation, and transcripts from this locus are

295   retained in the nucleus. Additionally, the locus contains a self-splicing site that produces a mature

11

296 transcript without additional machinery, allowing precise production of a mature sgRNA without any

297 unwanted extensions. Primer sequences for strain construction are listed in Supplementary File 2.

Yeast growth

299 The strains used in this study are listed in Supplementary File 3. Strains were grown to mid-log at

300 30°C in complete synthetic media lacking leucine (for dCas9 plasmid selection). For experiments

301 studying the *GAL1* locus, yeast were grown to mid-log in rich media (YP 2% D/YP 2% Gal) so that the

302 *GAL1* induction kinetics were similar to what we had observed previously (Murray et al., 2012,

303 2015). dCas9 expression was unaffected by the temporary absence of plasmid selection (Fig. 1 –

304 Figure Supplement 1).

Yeast growth controls

306 Assessment of growth in liquid culture (CSM-leucine) was achieved using a Bioscreen

307 spectrophotometer that automatically measures the optical density of cultures at 30°C every 20 min

308 for 24 h. Doubling times were extracted from the gradient of the curves during logarithmic growth.

Northern blotting

310 Northern blotting was performed as before (Murray et al., 2012; Nguyen et al., 2014) using

311 asymmetric PCR or *in vitro* transcription with T7 RNA polymerase to generate the radioactive strand-

312 specific probes for *GAL1* and *HMS2* respectively. Primers for these reactions are listed in

313 Supplementary File 4. Northern blots were quantified using ImageJ and images acquired using a

314 Phosphorimager. Images in the figures are scans of exposures to X-ray film.

Western blotting

316 dCas9 expression was confirmed after each experiment using an anti-Cas9 antibody (Diagenode

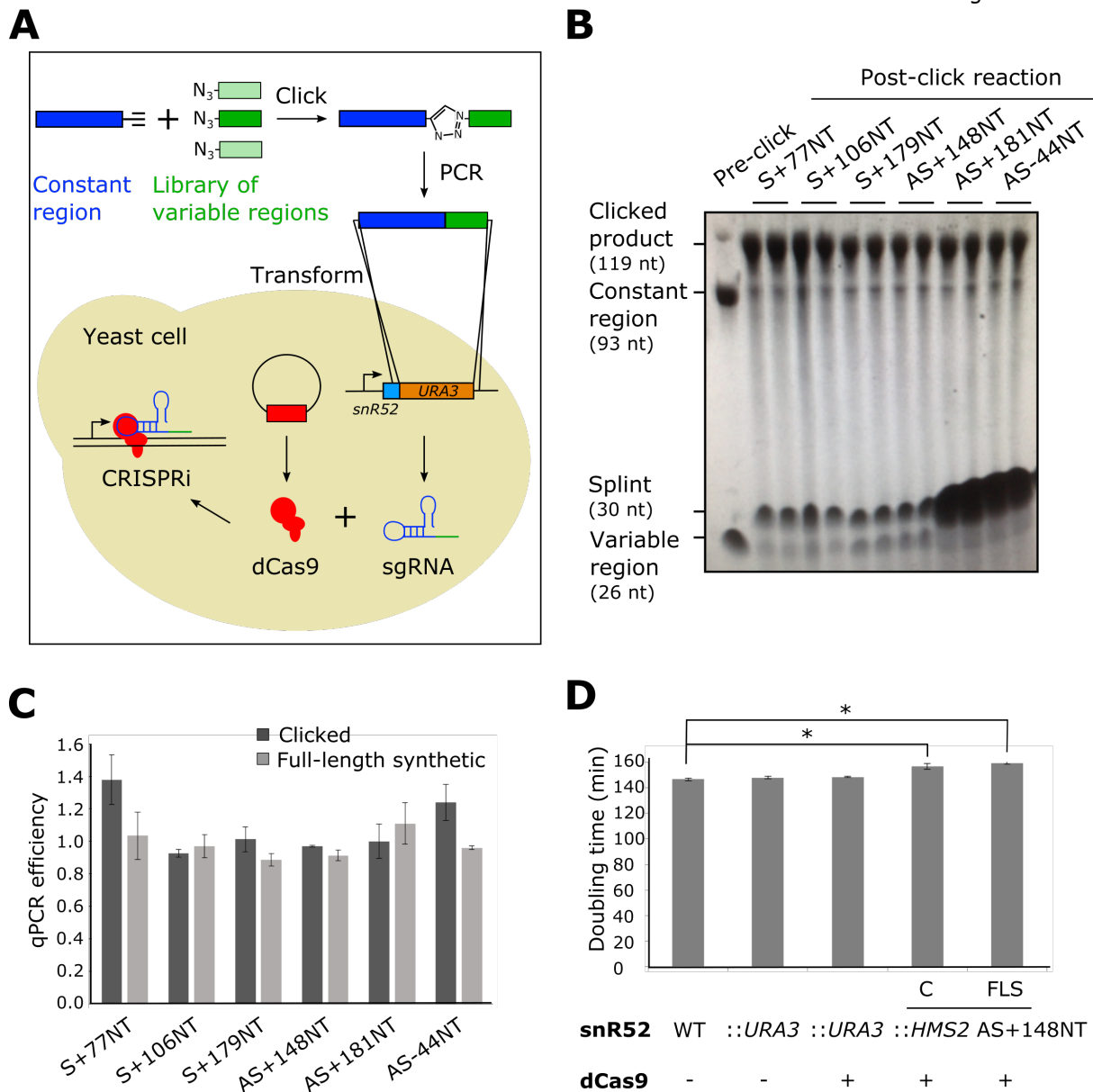317 C15310258) at 1:5000 dilution and anti-Tubulin (Abcam ab6160) at 1:3333.

3' RACE mapping

319 Mapping of the 3' end of the *GAL1* sense transcript was performed as (Nguyen et al., 2014). Primers

320 are listed in Supplementary File 5.

321   **FIGURED AND FIGURE LEGENDS**

322   **Figure 1. Experimental strategy for sgRNA template synthesis and incorporation into yeast.**

323

324   **A.** An outline of the experiment. Templates for sgRNA production were generated using a click

325   chemistry reaction between a single-stranded DNA oligonucleotide with a 3' alkyne group encoding

326   the constant region (dark blue) and a number of single-stranded DNA oligonucleotides with 5' azido

327   groups encoding the different variable regions (green). The resulting single-stranded DNA

328   oligonucleotide was purified, amplified by PCR and transformed into yeast to replace the *URA3*

329   selection cassette that had previously been introduced into the endogenous *snR52* locus. Correct

330   insertion was confirmed by Sanger sequencing. The expression of the sgRNA is driven from the

331   endogenous RNA polymerase III *snR52* promoter and processed to produce a mature sgRNA. The

13

332   sgRNA couples with enzymatically dead Cas9 (dCas9, red) expressed under the control of the *TDH3*

333   promoter off a plasmid to block transcription. See Methods for more detail. **B.** A polyacrylamide gel

334   visualised by UV shadowing reveals a high efficiency of the click reaction for all the *HMS2* constructs

335   (see Figures 2E and Figure 3 – Figure Supplement 1 for positions of the sgRNA binding sites). The

336   sizes of the variable region, DNA splint, constant region and clicked product are indicated. **C.** PCR

337   efficiencies of the clicked and full-length synthetic DNA oligonucleotides as measured by qPCR with a

338   serial dilution series. N=3, errors are standard error of the mean (SEM), all differences are not

339   significant p>0.05. **D.** Doubling times (min) of the indicated yeast strains grown in complete synthetic

340   media minus leucine. C, strains constructed using clicked oligonucleotides; FLS, strains constructed

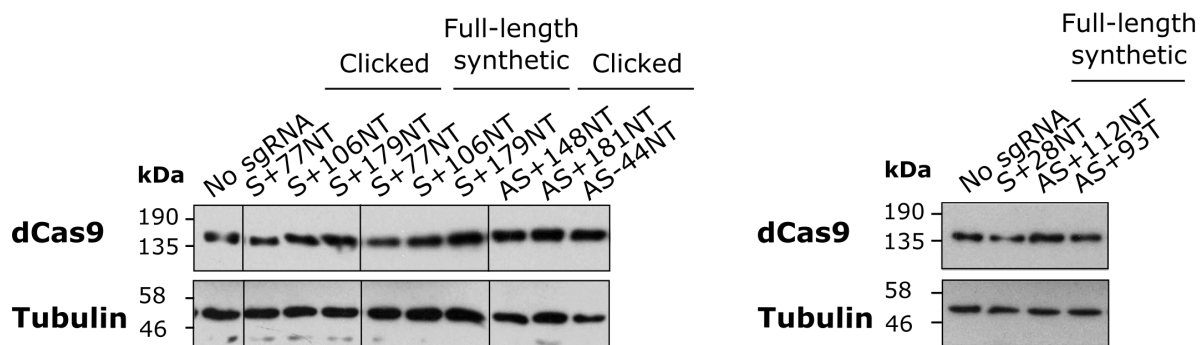341   using full-length synthetic oligonucleotides. N=10, errors are SEM, * p<0.05.

342

343   **Figure 1 - Figure Supplement 1. Levels of dCas9 protein in the experimental strains.**

Figure S1:

HMS2 strains: **GAL1 strains:**

345   A Western blot showing levels of dCas9 produced in the strains expressing the indicated sgRNAs

346   against *HMS2* (left panel) and *GAL1* (right panel). Tubulin levels are used as a loading control. Images

347   are taken from the same gels with the same exposure times but with some lanes spliced out

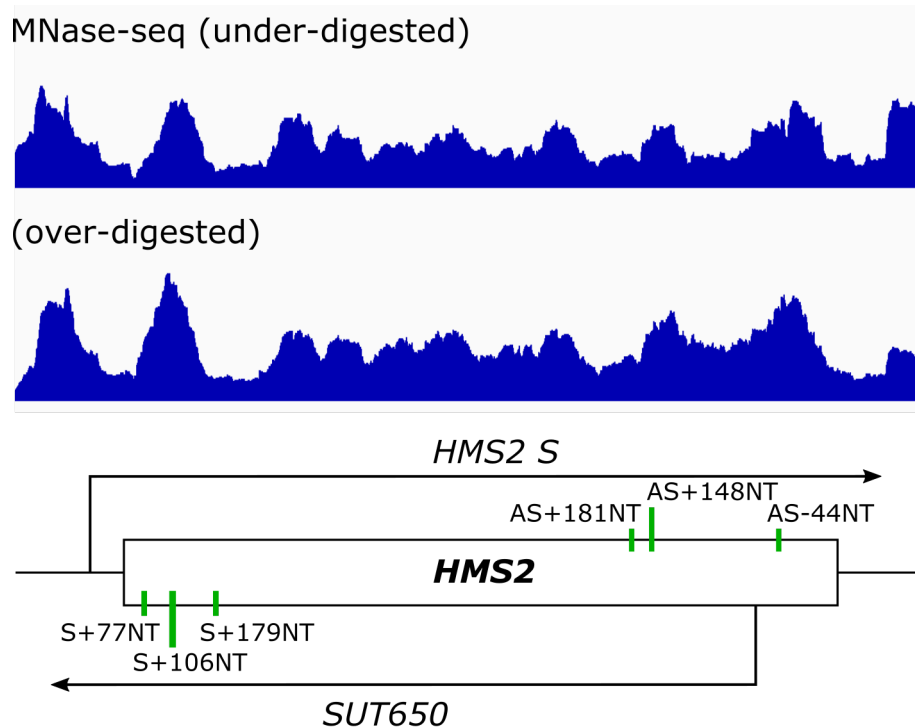348   (indicated with vertical lines).

349

350 **Figure 2. CRISPRi reduces antisense transcripts at *GAL1* and *HMS2*.**
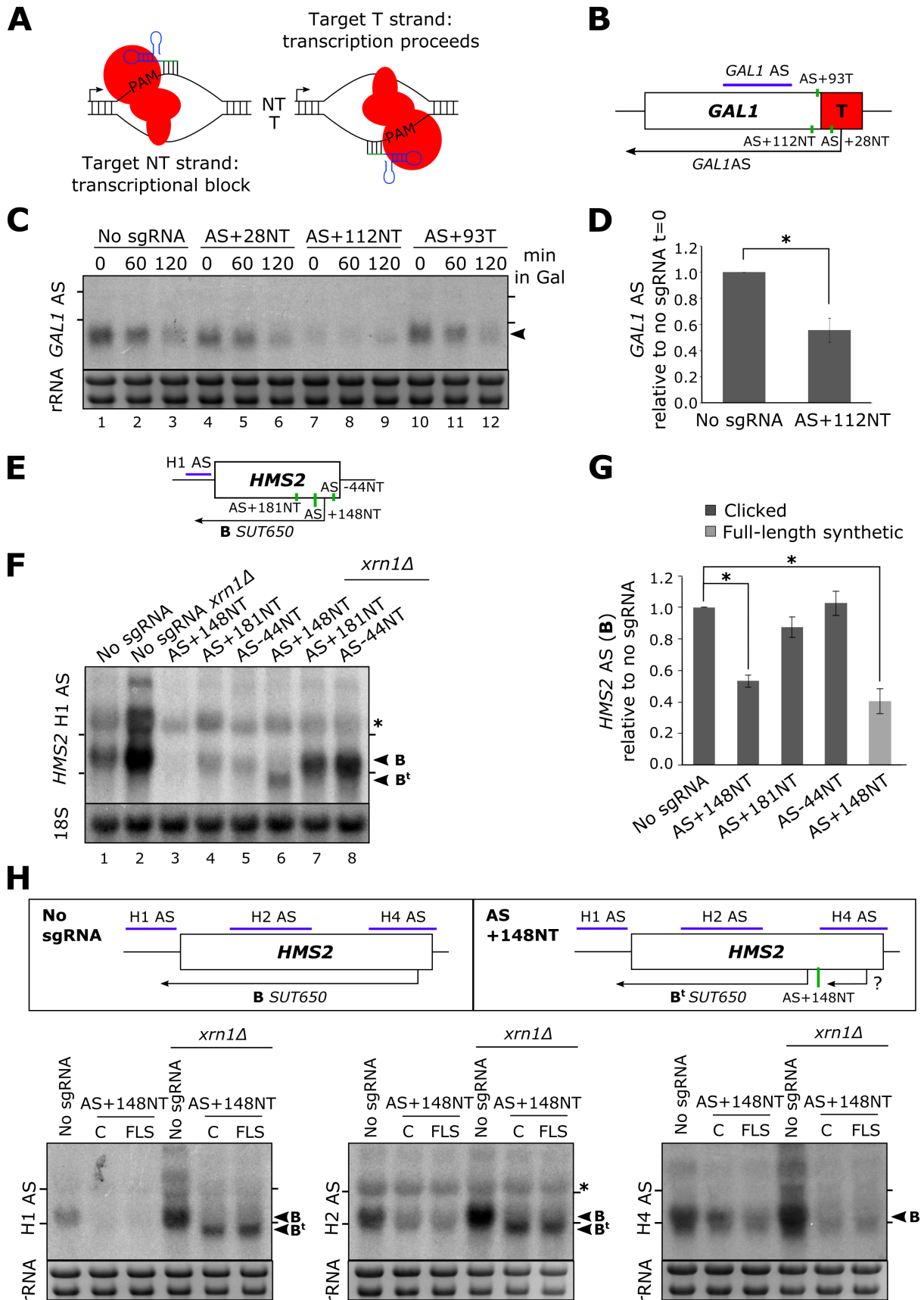
351

352   **A.** A schematic demonstrating the previously reported requirement of non-template strand targeting

353   by the sgRNA/dCas9 complex for strand-specific transcriptional repression. Arrows indicate the

354   direction of transcription. NT, non-template; T, template; red, dCas9; PAM, protospacer adjacent

355   motif; green/blue, sgRNA. **B.** A schematic of the engineered *GAL1* locus showing the site of insertion

356   of the *ADH1* terminator (T, red box), the transcription start site for the stable *GAL1* antisense

357   transcript and the positions of the designed sgRNAs (green vertical lines) targeting the non-template

358   (AS+28NT, AS+112NT) and template (AS+93NT) strands with respect to antisense transcription. The

359   position of the Northern blotting probe detecting the *GAL1* AS transcript is shown in purple. **C.** A

360   Northern blot showing the reduction in *GAL1* antisense transcript (black arrowhead) in the strain

361   expressing sgRNA AS+112NT/dCas9 relative to the no sgRNA control (*GAL1:ADH1*t *snR52::URA3* with

362   dCas9). sgRNAs AS+28NT and AS+93T do not alter *GAL1* AS levels. Samples were taken from cells

363   grown in glucose (t=0) and at the indicated times after transfer to galactose-containing media (min).

364   Positions of the rRNA are indicated by the short horizontal lines. Ethidium bromide-stained rRNA is

365   used as loading control. **D.** Quantification of Northern blotting for the *GAL1* AS transcript at t=0 in

366   the control no sgRNA strain and the strain with sgRNA AS+112NT. N=6, errors are SEM, * $p<0.05$. **E.** A

367   map of the *HMS2* locus showing the *HMS2* AS transcript, *SUT650* (black arrow, transcript B) and

368   positions of the three sgRNAs targeting *SUT650* (green vertical lines). The position of the Northern

369   blotting probe to detect *SUT650* (H1 AS) is shown by the purple line. **F.** A Northern blot probed with

370   *HMS2* antisense probe H1 (see schematic in (**E**)) showing the level of *SUT650* (black arrowhead,

371   transcript B) in the no sgRNA control (*snR52::URA3* with dCas9) strain and strains expressing the

372   indicated antisense-targeting sgRNAs. Deletion of *XRN1* allows detection of a shorter antisense

373   transcript (B^t) in the strain expressing AS+148NT. Positions of the rRNA are indicated by the short

374   horizontal lines. *represents cross-hybridisation with the 26S rRNA. A blot probed for the 18S rRNA

375   is used as loading control. **G.** Quantification of the level of *SUT650* (transcript B) reduction in the

376   strains expressing each of the 3 antisense sgRNAs relative to the control no sgRNA strain. N=4-8,

377   errors represent SEM, *$p<0.05$. Click-linked and full-length synthetic sgRNA AS+148NT templates

378   behave similarly. **H.** Northern blots with a series of *HMS2* antisense-specific probes. A new shorter

379   antisense transcript (B^t) can be detected upon *XRN1* deletion in the strains expressing sgRNA

380   AS+148NT/dCas9. Two clones of the CRISPRi strains produced using clicked (C) or full-length

381   synthetic (FLS) oligos for strain construction are shown. Positions of the antisense-specific probes

382   (purple) and the site of sgRNA AS+148NT/dCas9 binding (green vertical line) are shown in the

383   schematic. Positions of the rRNA on the Northern blot are indicated by the short horizontal lines.

384   *represents cross-hybridisation with the 26S rRNA. Ethidium bromide-stained rRNA is used as

385   loading control.

386 **Figure 2 - Figure Supplement 1**. **Nucleosome occupancy over the sgRNA target sites does not anti-**

387 **correlate with level of repression.**

MNase-seq (under-digested)

(over-digested)

HMS2 S

AS+148NT
AS+181NT   AS-44NT

HMS2

S+77NT   S+179NT
         S+106NT

SUT650

sgRNA	Relative nucleosome occupancy	
	Under	Over
S+77NT	4.295	14.17
S+106NT	16.04	33.99
S+179NT	9.391	11.51
AS+148NT	16.53	19.36
AS+181NT	11.97	15.09
AS-44NT	22.7	28.27

388

389 Nucleosome occupancy map for *HMS2* as measured by sequencing of a sample that has been under-

390 and over-digested with MNase (Knight et al., 2014). The schematic underneath shows the positions

391 of the sgRNA targeting sites. Relative nucleosome occupancy at each sgRNA site is shown in the

392 table for the under- and over-digested samples.

393

17

Figure 3. *HMS2* and *GAL1* sense transcripts are differently affected by blocking of their respective antisense transcripts.
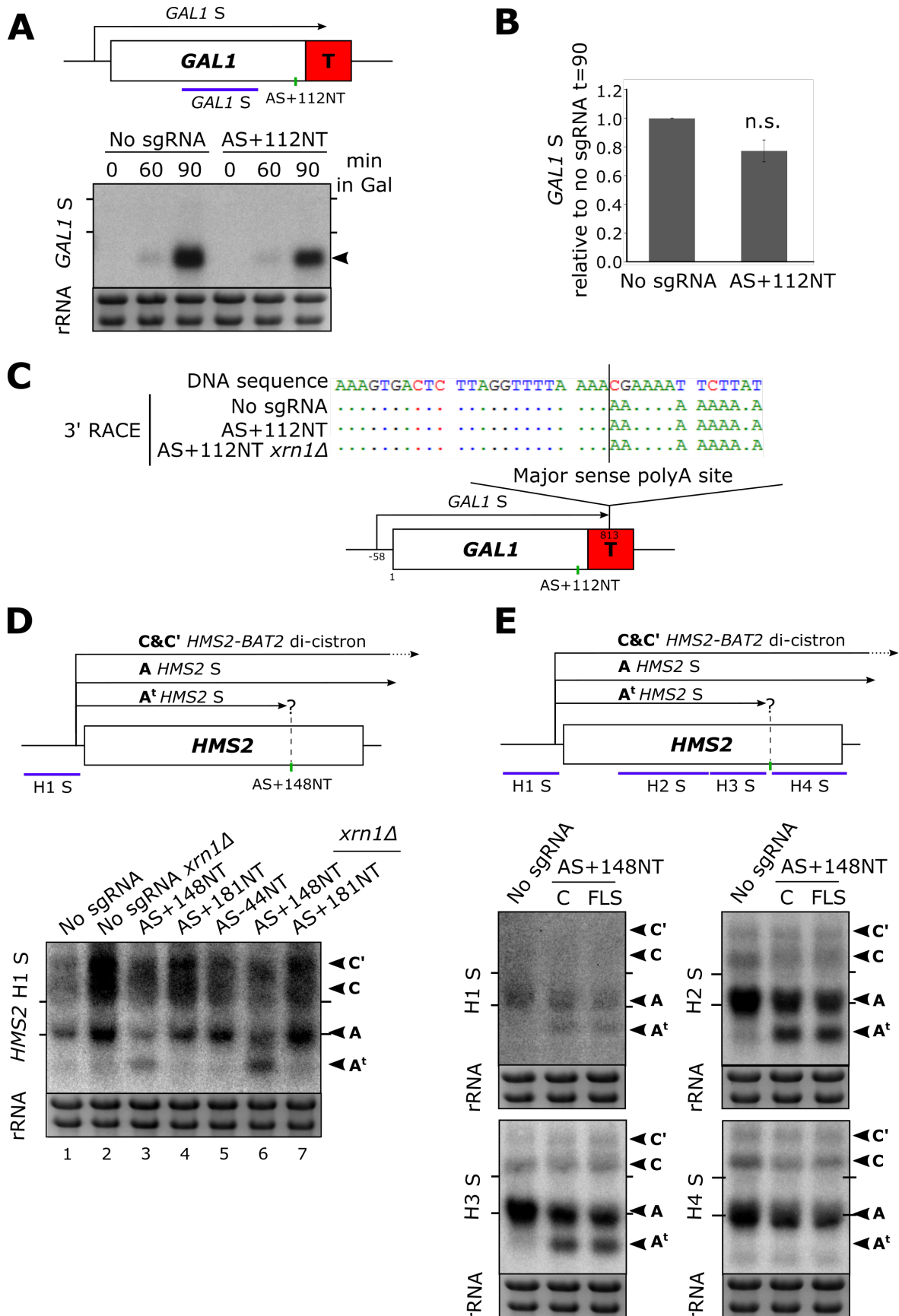
397   **A.** A Northern blot probed for the *GAL1* sense transcript (black arrow) in the control strain with no

398   sgRNA (*GAL1 ADH1*t *snR52::URA3* with dCas9) and in the strain expressing sgRNA AS+112NT/dCas9.

399   Samples were taken from cells grown in glucose (t=0) and at the indicated times after transfer to

400   galactose-containing media (min). Ethidium bromide-stained rRNA is used as a loading control. **B.**

401   Quantification of the Northern blot shown in (A) at t=90. N=4, error bars represent SEM, change is

402   statistically non-significant (n.s.) p=0.062. **C.** A schematic showing the results of *GAL1* sense

403   transcript 3' end mapping by RACE in the strains indicated. All distances are shown relative to the

404   sense TSS. Transcript cleavage and polyadenylation occurs beyond the position of the *GAL1* AS-

405   blocking AS+112NT sgRNA shown (green vertical line). **D.** A Northern blot probed with *HMS2* sense

406   probe H1 (purple) showing the level of *HMS2* sense (black arrowhead, transcript A) in the no sgRNA

407   control (*snR52::URA3* with dCas9) strain and strains expressing the indicated antisense-targeting

408   sgRNAs. A truncated sense transcript (A^t) was also detected in the strain expressing AS+148NT.

409   Positions of the rRNA are indicated by the short horizontal lines. Ethidium bromide-stained rRNA is

410   used as loading control. **E.** Northern blots with a series of *HMS2* sense-specific probes detecting the

411   regions indicated in the schematic. The position of the sgRNA AS+148NT/dCas9 binding site is shown

412   (green vertical line). Positions of the rRNA are indicated by the short horizontal lines. Ethidium

413   bromide-stained rRNA is used as loading control.

414

415 **Figure 3 - Figure Supplement 1.** *HMS2* sense-targeting sgRNAs/dCas9 do not affect *HMS2* sense or

416 **antisense transcript levels.**

Figure S3:
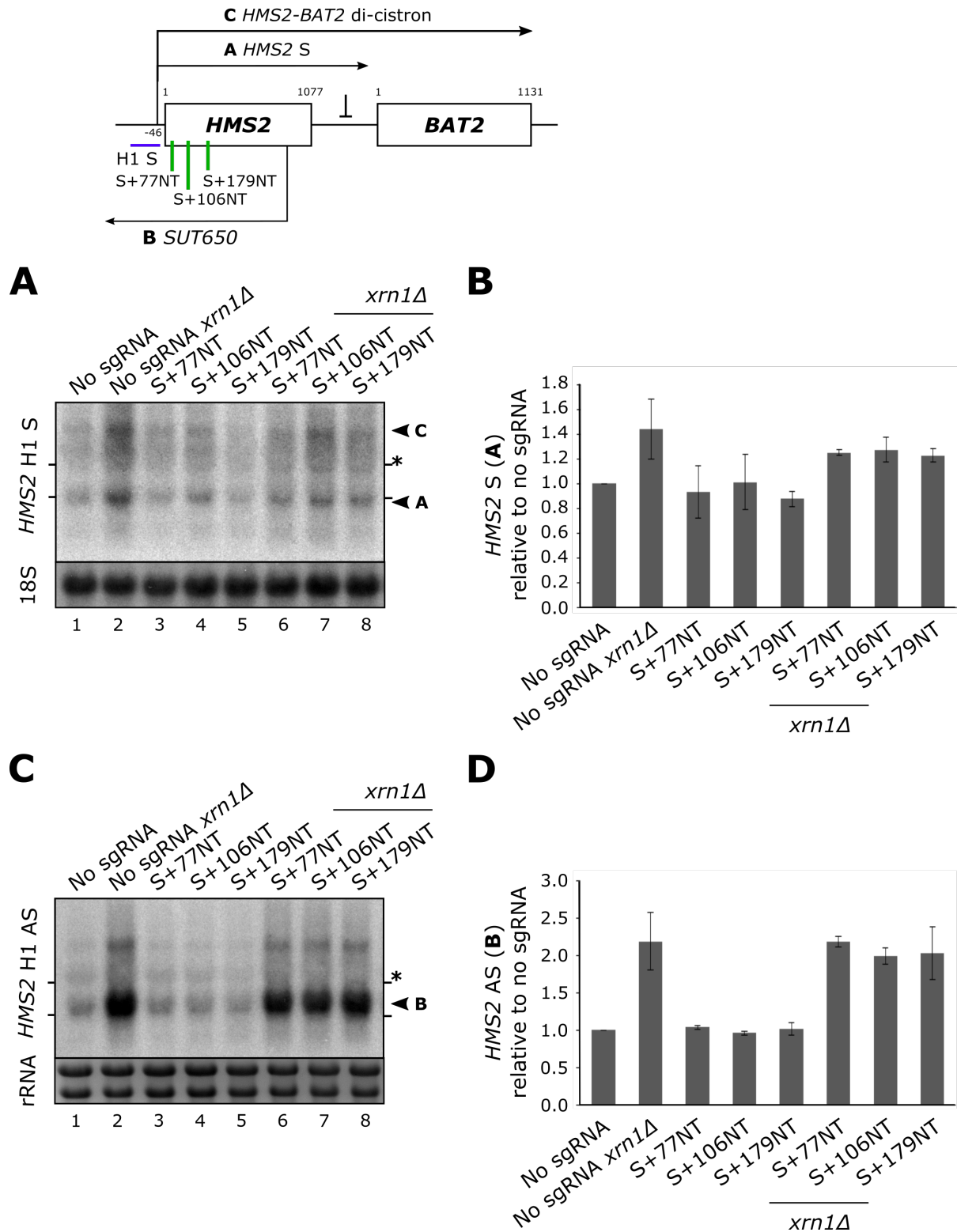
418 **A.** A Northern blot probed with *HMS2* sense probe H1 (purple) showing the level of *HMS2* sense

419 (black arrowhead, transcript A) in the no sgRNA control (*snR52::URA3* with dCas9) strain and strains

20

420   expressing the indicated sense-targeting sgRNAs. Positions of the rRNA are indicated by the short

421   horizontal lines. The 18S rRNA is used as loading control. *represents cross-hybridisation with the

422   26S rRNA. **B.** Quantification of the Northern blot in (A). N=2, errors represent the SEM. **C.** A Northern

423   blot as (A) but probed with *HMS2* antisense-specific probe H1. Ethidium bromide-stained rRNA is

424   used as loading control. **D.** Quantification of the Northern blot in (C). N=2, errors represent the SEM.

425

426 **Figure 4. CRISPRi block of *SUT650* and *GAL1* AS is not as efficient as previous genetic interventions.**
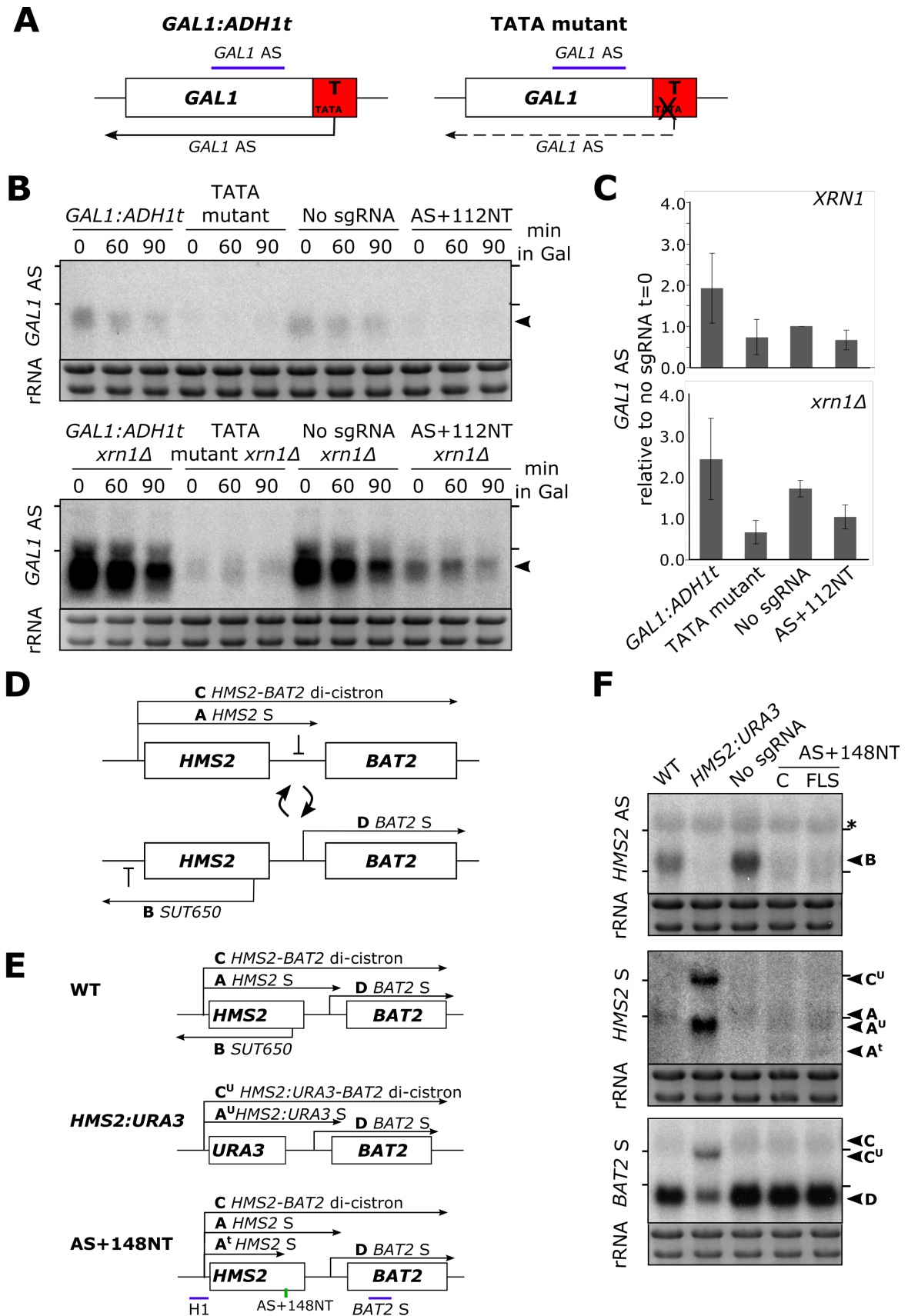
427

428 **A.** A schematic showing the previously used genetic intervention to repress the *GAL1* AS transcript

429 (Murray et al., 2015). In the TATA mutant construct, a TATA box within the engineered *ADH1*

430 terminator (T) is scrambled and the level of *GAL1* antisense transcript is reduced. **B.** A Northern blot

431 probed for the *GAL1* antisense transcript (black arrowhead) comparing the two methods of reducing

432 antisense at this locus in the presence (top blot) or absence (bottom blot) of *XRN1*. All samples were

433 run on the same gel and the blots were exposed to film for the same time. Samples were taken from

434 cells grown in glucose (t=0) and at the indicated times after transfer to galactose-containing media

435 (min). Positions of the rRNA are indicated by the short horizontal lines. Ethidium bromide-stained

436 rRNA is used as loading control. **C.** Quantification of the Northern blot in (B) at t=0. N=2, errors

437 represent the SEM. **D.** A schematic of the *HMS2-BAT2* locus, showing the *HMS2* sense and antisense

438 transcripts (A and B), the *HMS2-BAT2* di-cistronic transcripts (C and C') and the *BAT2* sense transcript

439 (D). Cells switch between sense- and antisense-dominant states in which the indicated transcripts

440 are produced (Nguyen et al., 2014). **E.** The *HMS2-BAT2* locus and associated transcripts in the WT

441 strain and strains that repress the *SUT650* transcript. In the *HMS2:URA3* strain, the entire coding

442 region of *HMS2* is replaced by that of *URA3*. **F.** Northern blots comparing the efficiency of *SUT650*

443 reduction by replacement of the *HMS2* coding region with that of *URA3* versus CRISPRi and the

444 relative effects of these two strategies on the *HMS2* sense and *BAT2* transcripts shown in (E). The

445 WT (BY4741) and *HMS2.URA3* strains have been transformed with plasmid pRS315 to allow for

446 growth on complete synthetic media lacking leucine and thus comparisons with the CRISPRi strains.

447 Positions of the rRNA are indicated by the short horizontal lines. *represents cross-hybridisation

448 with the 26S rRNA. Ethidium bromide-stained rRNA is used as loading control.

449

450

451

452 **Supplementary File 1. Templates for sgRNAs**

453 **Supplementary File 2. Primers for strain construction**

454 **Supplementary File 3. *Saccharomyces cerevisiae* strains used in this study**

455 **Supplementary File 4. Primers for construction of Northern blot probe templates**

456 **Supplementary File 5. Primers for 3' RACE mapping of the *GAL1* sense transcript**

457

23

458 **Supplementary File 1. Templates for sgRNAs**

sgRNA template	Sequence 5'-3'
Constant region	AGACATAAAAAACAAAAAAAGCACCACCGACTCGGTGCCACTTTTTCAAGTTGATAACGGACTAGCCTTATTTTAACTTGCTATTTCTAGCTC
HMS2 S+77NT variable region	TAAAACGATGTCTTTGTAAGCAAACT
HMS2 S+106NT variable region	TAAAACGCTGCAGGGGAACGCTTACT
HMS2 S+179NT variable region	TAAAACGACCAGTTCACCAAAGTCAT
HMS2 AS+148NT variable region	TAAAACCGGGATGCAACTGCGGGTGC
HMS2 AS+181NT variable region	TAAAACTATCCAAAGAGCAGTTCATA
HMS2 AS-44NT variable region	TAAAACACTGCAAAAAATGGTGGAAA
HMS2 S+77NT full-length	AGACATAAAAAACAAAAAAAGCACCACCGACTCGGTGCCACTTTTTCAAGTTGATAACGGACTAGCCTTATTTTAACTTGCTATTTCTAGCTCTAAAACGATGTCTTTGTAAGCAAACT
HMS2 S+106NT full-length	AGACATAAAAAACAAAAAAAGCACCACCGACTCGGTGCCACTTTTTCAAGTTGATAACGGACTAGCCTTATTTTAACTTGCTATTTCTAGCTCTAAAACGCTGCAGGGGAACGCTTACT
HMS2 S+179NT full-length	AGACATAAAAAACAAAAAAAGCACCACCGACTCGGTGCCACTTTTTCAAGTTGATAACGGACTAGCCTTATTTTAACTTGCTATTTCTAGCTCTAAAACGACCAGTTCACCAAAGTCAT
HMS2 AS+148NT full-length	AGACATAAAAAACAAAAAAAGCACCACCGACTCGGTGCCACTTTTTCAAGTTGATAACGGACTAGCCTTATTTTAACTTGCTATTTCTAGCTCTAAAACCGGGATGCAACTGCGGGTGC
HMS2 AS+181NT full-length	AGACATAAAAAACAAAAAAAGCACCACCGACTCGGTGCCACTTTTTCAAGTTGATAACGGACTAGCCTTATTTTAACTTGCTATTTCTAGCTCTAAAACTATCCAAAGAGCAGTTCATA
HMS2 AS-44NT full-length	AGACATAAAAAACAAAAAAAGCACCACCGACTCGGTGCCACTTTTTCAAGTTGATAACGGACTAGCCTTATTTTAACTTGCTATTTCTAGCTCTAAAACACTGCAAAAAATGGTGGAAA
GAL1 AS+28NT full-length	CAAATTTTAAAGTGACTCTTGTTTTAGAGCTAGAAATAGCAAGTTAAAATAAGGCTAGTCCGTTATCAACTTGAAAAAGTGGCACCGAGTCGGTGGTGCTTTTTTTGTTTTTTATGTCT
GAL1 AS+112NT full-length	TGAGTTCAAACCGCAGTTGAGTTTTAGAGCTAGAAATAGCAAGTTAAAATAAGGCTAGTCCGTTATCAACTTGAAAAAGTGGCACCGAGTCGGTGGTGCTTTTTTTGTTTTTTATGTCT
GAL1 AS+93T full-length	TTTTCATGGTTTTTTAATTGGTTTTAGAGCTAGAAATAGCAAGTTAAAATAAGGCTAGTCCGTTATCAACTTGAAAAAGTGGCACCGAGTCGGTGGTGCTTTTTTTGTTTTTTATGTCT

459

460

24

461   **Supplementary File 2. Primers for strain construction**

Primer	Sequence 5'-3'
URA3 insertion into *SNR52* F (template = pRS316)	GATGAATGACATTAGCGTGAACAATCTCTGATACAAAA TCCTGAGAGTGCACCACGCTTT
URA3 insertion into *SNR52* R (template = pRS316)	CAGAAGGAAGGCAACATAAGTTTTTCTAATCCTAAAAT CTGTGCGGTATTTCACACCGCA
sgRNA *HMS2* S+77NT insertion into *SNR52* F	TCGGCGTTCGAAACTTCTCCGCAGTGAAAGATAAATGA TCAGTTTGCTTACAAAGACATC
sgRNA *HMS2* S+106NT insertion into *SNR52* F	TCGGCGTTCGAAACTTCTCCGCAGTGAAAGATAAATGA TCAGTAAGCGTTCCCCTGCAGC
sgRNA *HMS2* S+179NT insertion into *SNR52* F	TCGGCGTTCGAAACTTCTCCGCAGTGAAAGATAAATGA TCATGACTTTGGTGAACTGGTC
sgRNA *HMS2* AS+148NT insertion into *SNR52* F	TCGGCGTTCGAAACTTCTCCGCAGTGAAAGATAAATGA TCGCACCCGCAGTTGCATCCCG
sgRNA *HMS2* AS+181NT insertion into *SNR52* F	TCGGCGTTCGAAACTTCTCCGCAGTGAAAGATAAATGA TCTATGAACTGCTCTTTGGATA
sgRNA *HMS2* AS-44NT insertion into *SNR52* F	TCGGCGTTCGAAACTTCTCCGCAGTGAAAGATAAATGA TCTTTCCACCATTTTTTGCAGT
sgRNA *GAL1* AS+28NT insertion into *SNR52* F	TCGGCGTTCGAAACTTCTCCGCAGTGAAAGATAAATGA TCCAAATTTT AAAGTGACTCTTG
sgRNA *GAL1* AS+112NT insertion into *SNR52* F	TCGGCGTTCGAAACTTCTCCGCAGTGAAAGATAAATGA TCTGAGTTCAAACCGCAGTTGA
sgRNA *GAL1* AS+93T insertion into *SNR52* F	TCGGCGTTCGAAACTTCTCCGCAGTGAAAGATAAATGA TCTTTTCATG GTTTTTTAATTGG
sgRNA insertion into *SNR52* R	AGAGGTGGCATTTTACATAACAATAGTGACAAAAAATA AAAGACATAAAAAACAAAAAAA
SNR52 check F	AGCAAACAGCCACTGACTGT
SNR52 check R	GCGTACTAATGTTTTTTGTT
SNR52 Sequencing F	TTGTAGTGCCCTCTTGGGCTAG

462

463

464   **Supplementary File 3.** *Saccharomyces cerevisiae* **strains used in this study**

Strain name	Parent	Genotype	Source
BY4741	S288C	MATa; *his3Δ 1; leu2Δ 0; met15Δ 0; ura3Δ*	Euroscarf
snR52::URA3 + dCas9	BY4741	snR52::*URA3* + p*TDH3*-dCas9 (Addgene plasmid 46920, *LEU*)	This study
HMS2 S+77NT	snR52::URA3 +dCas9	snR52::sgRNA *HMS2* S+77NT	This study
HMS2 S+106NT	snR52::URA3 +dCas9	snR52::sgRNA *HMS2* S+106NT	This study
HMS2 S+179NT	snR52::URA3 +dCas9	snR52::sgRNA *HMS2* S+179NT	This study
HMS2 AS+148NT	snR52::URA3 +dCas9	snR52::sgRNA *HMS2* AS+148NT	This study
HMS2 AS+181NT	snR52::URA3 +dCas9	snR52::sgRNA *HMS2* AS+181NT	This study
HMS2 AS-44NT	snR52::URA3 +dCas9	snR52::sgRNA *HMS2* AS-44NT	This study
HMS2 S+77NT *xrn1*	*HMS2* S+77NT	*xrn1*::HISMX6	This study
HMS2 S+106NT *xrn1*	*HMS2* S+106NT	*xrn1*::HISMX6	This study
HMS2 S+179NT *xrn1*	*HMS2* S+179NT	*xrn1*::HISMX6	This study
HMS2 AS+148NT *xrn1*	*HMS2* AS+148NT	*xrn1*::HISMX6	This study
HMS2 AS+181NT *xrn1*	*HMS2* AS+181NT	*xrn1*::HISMX6	This study
HMS2 AS-44NT *xrn1*	*HMS2* AS-44NT	*xrn1*::HISMX6	This study
BY4741 pRS315	BY4741	+pRS315 (*LEU*)	This study
HMS2:URA3	BY4741	*HMS2 Δ(1-1076)::URA3*	(Nguyen et al., 2014)
HMS2:URA3 pRS315	*HMS2:URA3*	+pRS315 (*LEU*)	This study
*GAL1::ADH1*t	BY4741	*GAL1 Δ(758-1587)::ADH1*t	(Murray et al., 2012)
TATA mutant	BY4741	*GAL1 Δ(758-1587)::ADH1*t (scramble TATA #1)	(Murray et al., 2015)
*GAL1::ADH1*t *xrn1*	*GAL1::ADH1*t	*xrn1::KANMX6*	This study
TATA mutant *xrn1*	TATA mutant	*xrn1::HISMX6*	This study
*GAL1::ADH1*t snR52::URA3 +dCas9	*GAL1::ADH1*t	snR52::*URA3* + p*TDH3*-dCas9 (Addgene plasmid 46920, *LEU*)	This study
GAL1 AS+28NT	*GAL1::ADH1*t snR52::URA3	snR52::sgRNA *GAL1* AS+28NT	This study
GAL1 AS+112NT	*GAL1::ADH1*t snR52::URA3 + dCas9	snR52::sgRNA *GAL1* AS+112NT	This study
GAL1 AS+93T	*GAL1::ADH1*t snR52::URA3 +dCas9	snR52::sgRNA *GAL1* AS+93T	This study
GAL1 AS+112NT *xrn1*	*GAL1* AS+112NT	*xrn1::KANMX6*	This study

465

466

26

467 **Supplementary File 4. Primers for construction of Northern blot probe templates**

Primer	Sequence 5'-3'
HMS2 H1 S F	GACCCGTCCTTCTTTTACCC
HMS2 H1 S T7 R	TAATACGACTCACTATAGGGAGAGACACACTTGGCGACTG
HMS2 H1 AS T7 F	TAATACGACTCACTATAGGGGACCCGTCCTTCTTTTACCC
HMS2 H1 AS R	AGAGACACACTTGGCGACTG
HMS2 H2 S F	GGCGGGCCGCCCGGACTGCG
HMS2 H2 S T7 R	TAATACGACTCACTATAGGGCGGTTTGGTAGGCGTGAAAC
HMS2 H2 AS T7 F	TAATACGACTCACTATAGGGGGCGGGCCGCCCGGACTGCG
HMS2 H2 AS R	CGGGTGCCACTGAGTGGCCG
HMS2 H3 S F	GTTTCA CGCCTACCAA ACCG
HMS2 H3 S T7 R	TAATACGACTCACTATAGGGCGGGTGCCACTGAGTGGCCG
HMS2 H4 S F	TACGACCTTC TTTTCGTCAC
HMS2 H4 S T7 R	TAATACGACTCACTATAGGGCGGGTGCCACTGAGTGGCCG
HMS2 H4 AS T7 F	TAATACGACTCACTATAGGGTACGACCTTC TTTTCGTCAC
HMS2 H4 AS R	GAATGACCCTCAGAGGCAGG
BAT2 S F	AGGCTTACAGAACGGTGGAC
BAT2 S T7 R	TAATACGACTCACTATAGGGGCTCTATCAGGCGTGGAAAC
GAL1 F	TGTGTCGGACTGGTCTAATT
GAL1 R	GATCCATACCGCCATTGTTA
18S F	AGTGAAACTGCGAATGGCTC
18S R	TGCTGGCACCAGACTTGCCC

468

469

470

471 **Supplementary File 5. Primers for 3' RACE mapping of the *GAL1* sense transcript**

Primer	Sequence 5'-3'
Adapter Primer (AP)	GCCCACGCGTCGACTAGTACTTTTTTTTTTTTTTTTT
Universal amplification primer (UAP)	GCCCACGCGTCGACTAGTAC
GAL1 +346 F	TTGATCCTTCTGTGTCGGACTG

472